

Lattice Boltzmann method for gaseous microflows using kinetic theory boundary conditions

G. H. Tang,^{a)} W. Q. Tao, and Y. L. He

State Key Laboratory of Multiphase Flow, School of Energy and Power Engineering,
Xi'an Jiaotong University, Xi'an, Shaanxi 710049, People's Republic of China

(Received 15 December 2004; accepted 22 February 2005; published online 22 April 2005)

The lattice Boltzmann method is developed to study gaseous slip flow in microchannels. An approach relating the Knudsen number with the relaxation time in the lattice Boltzmann evolution equation is proposed by using gas kinetic equation resulting from the Bhatnagar–Gross–Krook collision model. The slip velocity at the solid boundaries is obtained with kinetic theory boundary conditions. The two-dimensional micro-Couette flow, micro-Poiseuille flow, and micro-lid-driven cavity flow are simulated using the present model. It is found that the numerical results agree well with available analytical and benchmark solutions. © 2005 American Institute of Physics.

[DOI: 10.1063/1.1897010]

Microelectromechanical systems technology has been developed rapidly in recent years. As the scale of the domain is reduced, the continuum assumption is no longer applicable.¹ The Knudsen number Kn , which is defined as $Kn = \lambda/H$, provides a direct means of validating the continuum approach as it compares the mean free path λ to the characteristic length H . For $Kn > 10$ the system can be considered to be a free molecular flow. A flow is considered as a continuum for $Kn < 0.001$. The intermediate values of $0.1 < Kn < 10$ are associated with a transition flow regime while those within the range of $0.001 < Kn < 0.1$ are representative of a slip flow regime. The Navier–Stokes equation may be applied to flows within the slip regime or marginally transitional if the first-order or higher-order velocity slip boundary conditions are employed at the wall. For flows in the high transition or free molecular regimes the problem requires direct solution of the full Boltzmann equation or a gas dynamic model such as the direct simulation Monte Carlo (DSMC).

In the last decade or so, the lattice gas automata and its later derivative, the lattice Boltzmann method (LBM) have emerged as new and effective numerical approaches of computational fluid dynamics and have achieved considerable success in simulating fluid flows and associated transport phenomena, especially for complicated boundaries such as porous media flow.² Though analytical approaches and traditional numerical methods mentioned above have been usually used for microchannel flow investigation, most of the studies are limited to simple geometries such as circular tubes or parallel channels. Therefore, it is quite necessary to develop the lattice Boltzmann method for microflow simulation. In this Brief Communication, we simulate microflows with the lattice Boltzmann model by applying kinetic theory boundary conditions. The boundary conditions for the discrete lattice Boltzmann model will be briefly discussed. Numerical simulations for three generalized problems will be carried out to test the validity of the approach.

The basic discrete-velocity Boltzmann kinetic equation is³

$$f_i(\mathbf{r} + \mathbf{c}_i \Delta t, t + \Delta t) - f_i(\mathbf{r}, t) = -\frac{\Delta t}{\tau + 0.5 \Delta t} [f_i(\mathbf{r}, t) - f_i^{eq}(\mathbf{r}, t)], \quad (1)$$

where f is the single particle density distribution function, τ is the collision relaxation time, and Δx and Δt are the lattice constant and the time step size, respectively. The local equilibrium f_i^{eq} is the conditional minimizer of the entropy function H and the expression for D2Q9 model can be found in Refs. 3–7.

The discrete-velocity set on the D2Q9 lattice structure is $\mathbf{c}_0 = 0$, $\mathbf{c}_i = \{\cos[(i-1)\pi/2], \sin[(i-1)\pi/2]\}c$ for $i = 1, 2, 3, 4$, and $\mathbf{c}_i = \{\cos[(i-5)\pi/2 + \pi/4], \sin[(i-5)\pi/2 + \pi/4]\}c$ for $i = 5, 6, 7, 8$, where $c = \Delta x/\Delta t$. Furthermore, the characteristic speed c is related to the reference temperature by the relation $c = \sqrt{3RT}$. The macroscopic variables for the fluid mass density, the fluid momentum, and pressure are defined by $\rho = \sum_i f_i$, $\rho \mathbf{u} = \sum_i f_i \mathbf{c}_i$, and $p = \rho c^2/3$.

It is known that the Chapman–Enskog solution of the Bhatnagar–Gross–Krook (BGK) equation yields the Navier–Stokes equation of macroscopic gas dynamics with the expression of dynamic viscosity,⁸

$$\eta = \frac{nk_B T}{\nu} = \frac{p}{\nu}, \quad (2)$$

where n denotes the number of molecules per unit volume of gas and k_B is called the Boltzmann constant. The collision frequency ν is defined as the ratio of mean molecular thermal speed \bar{c} to the mean free path λ ,

$$\nu = \bar{c}/\lambda \quad (3)$$

and \bar{c} is given by⁸

^{a)} Author to whom correspondence should be addressed. Telephone: 86-29-82663481. Fax: 86-29-82669106. Electronic mail: ghtang@xjtu.edu.cn

$$\bar{c} = \sqrt{\frac{8RT}{\pi}}, \quad (4)$$

where $R=k_B/m$ is the gas constant and m is the molecule mass. For uniform mesh, we have $H=N_H\Delta x$, where N_H is the characteristic lattice number. Combining Eqs. (3) and (4), together with $c=\Delta x/\Delta t$, $c=\sqrt{3RT}$ and $H=N_H\Delta x$, we can obtain

$$\text{Kn} = \frac{\lambda}{H} = \frac{\sqrt{8/3\pi}}{\nu N_H \Delta t}. \quad (5)$$

In the BGK model the local relaxation time $\tau=1/\nu$. Using the relaxation time to replace ν in Eq. (5), we have

$$\frac{\tau}{\Delta t} = \frac{N_H \text{Kn}}{\sqrt{8/3\pi}}. \quad (6)$$

Finally, we can relate the Knudsen number to the relaxation time in the lattice Boltzmann evolution equation by the following expression approximately for simplicity:

$$\frac{\tau}{\Delta t} = N_H \text{Kn}. \quad (7)$$

If τ is known, by Eq. (2) we can obtain the gas dynamic viscosity.

Bounce-back or modified bounce-back treatment at the solid boundaries is usually used in the lattice Boltzmann method to get the nonslip boundary conditions for continuum flows.⁹ To capture the gas slip velocity in the microflows, bounce-back and specular reflection conditions are combined in Ref. 10. In this Brief Communication, we use the discrete kinetic theory boundary conditions to get the slip velocity at the solid boundaries.

In the framework of classical kinetic theory of fluids, the Maxwell boundary conditions are defined as the ones of a gas which reemitted by a solid wall either with specular or with diffusive reemission law. In order to obtain a satisfactory reflection law the following notation will be needed.

A wall $\partial\Omega$ is completely specified at any point P . At time t , its position is $\mathbf{r}(\mathbf{r} \in \partial\Omega)$, and \mathbf{n} is the inward-pointing unit vector normal to the boundary surface, at P . \mathbf{u}_w is the velocity of the wall at P . Thus we shall denote the distribution function in a frame of reference moving with the wall velocity as $f(\xi)$, with $\xi=\mathbf{c}-\mathbf{u}_w$.

We assume that the gas is composed of identical particles with velocities restricted to a given finite set of $2N$ vectors and arrange given velocities into three groups. I_i denotes the set of velocity numbers i such that $(\mathbf{c}_i-\mathbf{u}_w)\mathbf{n}<0$, which represent incident molecules. Similarly, I_r denotes the set of indices such that $(\mathbf{c}_i-\mathbf{u}_w)\mathbf{n}>0$, the reflected molecules, and for the molecules having a velocity such that $(\mathbf{c}_i-\mathbf{u}_w)\mathbf{n}=0$ we introduce their index set I_g , representing the grazing molecules at the wall. Then, one can characterize the gas-surface interaction on the wall as

$$\forall j \in I_r, \quad (\xi_j\mathbf{n})f(\xi_j) = \sum_{i \in I_i} -(\xi_i\mathbf{n})R_{ij}f(\xi_i), \quad (8)$$

where $R_{ij} \geq 0$ is the transition probability density that a particle with velocity ξ_i , $\xi_i\mathbf{n}<0$ hitting the wall is instantaneously

reflected with velocity ξ_j , $\xi_j\mathbf{n}>0$. If the wall is nonporous and nonadsorbing, the non-negative R_{ij} must satisfy the normalization condition:

$$\forall i \in I_i, \quad \sum_{j \in I_r} R_{ij} = 1. \quad (9)$$

If it is assumed that a fraction σ_ν ($0 \leq \sigma_\nu \leq 1$) of the molecules is reemitted diffusively from the surface, while the fraction $(1-\sigma_\nu)$ is reflected in a specular fashion (according to the rarefied gas dynamics, σ_ν is called the tangential momentum accommodation coefficient), we can specify the coefficients $R_{i,j}$ and rewrite Eq. (8) as

$$\forall j \in I_r, \quad (\xi_j\mathbf{n})f(\xi_j) = (1-\sigma_\nu)f(\xi_{j'}) (\xi_j\mathbf{n}) + \sigma_\nu R_j^D \sum_{i \in I_i} -(\xi_i\mathbf{n})f(\xi_i), \quad (10)$$

where R_j^D is the purely diffusive part and $\xi_j-\xi_{j'}=2(\xi_j\mathbf{n})\mathbf{n}$. R_j^D does not depend on the incident directions i because a particle which is reflected diffusively has completely lost its memory about the incoming stream. The detailed solving process of R_j^D for the lattice Boltzmann method can see Ref. 11, in which completely diffusive boundary conditions are applied for continuum flow simulation. In addition, it should be noted that such boundary conditions like Eq. (10) were presented by Gatignol,¹² Cercignan,¹³ and Preziosi and Longo¹⁴ for discrete Boltzmann equation models. Therefore, the unknown particle distribution function $f(\mathbf{r}, \mathbf{c}_j, t+\Delta t)$ at the boundaries during the lattice Boltzmann equation evolution process can be calculated using the following equation:

$$\forall j \in I_r, \quad f(\mathbf{r}, \mathbf{c}_j, t+\Delta t) = (1-\sigma_\nu)f(\mathbf{r}, \mathbf{c}_{j'}, t+\Delta t) (\xi_j\mathbf{n}) + \sigma_\nu \frac{\sum_{i \in I_i} -(\xi_i\mathbf{n})f(\mathbf{r}, \mathbf{c}_i, t+\Delta t)}{\sum_{j \in I_r} (\xi_j\mathbf{n})f^{\text{eq}}(\mathbf{r}, \mathbf{c}_j, \rho_w, \mathbf{u}_w)} \times f^{\text{eq}}(\mathbf{r}, \mathbf{c}_j, \rho_w, \mathbf{u}_w). \quad (11)$$

Note that for most gas-surface interactions at engineering conditions, the diffusive boundary condition is appropriate. However, the accommodation coefficient depends on the fluid and the surface conditions and has ever been observed experimentally to be as low as 0.2.¹ For this reason, a study involving the incompletely diffusive reflection ($\sigma_\nu \neq 1$) is necessary.

We apply the present model to the micro-Couette flow first. Two infinite parallel plates are separated by a distance H . The upper plate at $y=H$ moves at a constant velocity u_0 while the lower plate is at rest. In the simulations, the lattice used is a 80×80 square mesh, and the velocity of the upper plate is $u_0=0.001$. Periodic boundary conditions are applied at the channel inlet and outlet. Note that analytical results by solving the Navier-Stokes equation with slip boundary conditions are in good agreement with the solutions of the linearized Boltzmann equation in the slip regime.¹ For simplic-

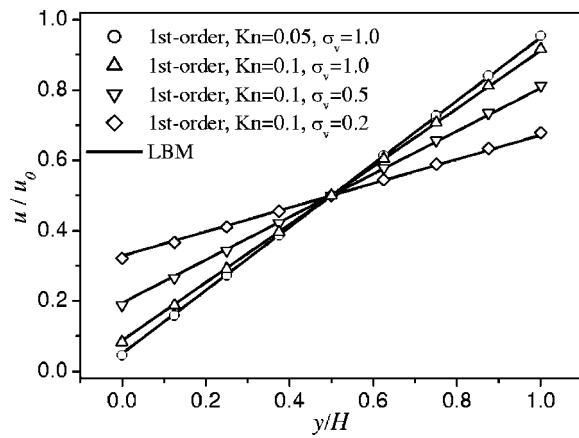


FIG. 1. Comparisons of the present LBM model and first-order analytical solutions for micro-Couette flow. Open symbols represent analytical solutions and solid lines represent the LBM results.

ity, the following linear velocity profile from first-order slip boundary condition is used here for comparison:¹

$$\frac{u}{u_0} = \frac{y/H + \text{Kn}(2 - \sigma_v)/\sigma_v}{1 + 2\text{Kn}(2 - \sigma_v)/\sigma_v}. \quad (12)$$

Figure 1 shows the velocity profiles along the y direction. The slip velocity at the lower wall can be clearly observed in the figure if the Knudsen number is not zero. As the Knudsen number increases or the tangential momentum accommodation coefficient decreases, the slip velocity at the lower wall gets larger. The LBM simulation results are in good agreement with the first-order analytical solutions of the Navier–Stokes equation.

Second, the micro-Poiseuille flow is also studied with this model. The two-dimensional channel of length L extends from $y=0$ to $y=H$ ($L=10H$). The upper plate and lower plate remain stationary. The channel inlet is given uniform velocity at $u_0=0.001$. The mesh size of 1500×150 is used in the simulation.

The channel outlet values of the friction constant ($C_f \text{Re}$) by using different approaches are listed in Table I. In this table, the friction constant by the first-order solution,¹

TABLE I. Comparisons of friction constants ($C_f \text{Re}$) at the channel outlet between first-order, second-order solutions, and present LBM results.

Kn	σ_v	$C_f \text{Re}$ (First order)	$C_f \text{Re}$ (Second order)	$C_f \text{Re}$ (LBM)
0.01	1.0	22.64	22.49	22.21
0.01	0.8	22.02	21.81	21.40
0.01	0.5	20.34	19.99	19.34
0.05	1.0	18.46	17.88	17.82
0.05	0.8	16.55	15.91	15.91
0.05	0.5	12.63	11.95	12.02
0.1	1.0	15.00	14.09	14.10
0.1	0.8	12.63	11.79	11.93
0.1	0.5	8.57	7.91	8.16

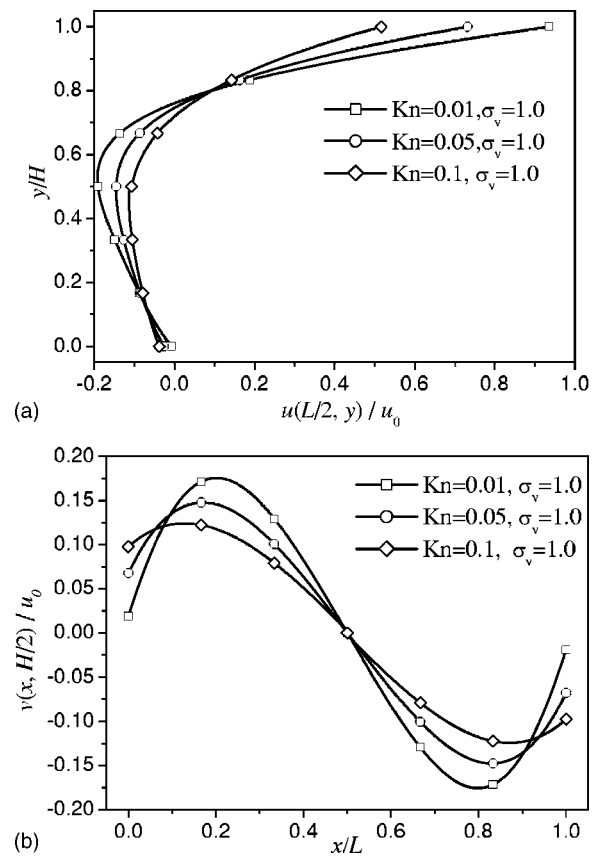


FIG. 2. The Knudsen number effect on the velocity profiles through the cavity center at $\text{Re}=0.3$. (a) u velocity along the vertical centerline of the cavity. (b) v velocity along the horizontal centerline of the cavity.

$$C_f \text{Re} = \frac{24}{1 + 6\text{Kn}(2 - \sigma_v)/\sigma_v} \quad (13)$$

and second-order solution¹⁵ are used for comparison,

$$C_f \text{Re} = \frac{24}{1 + 6\alpha\text{Kn}(2 - \sigma_v)/\sigma_v + 12\beta\text{Kn}^2}, \quad (14)$$

where $\alpha=1.11$ and $\beta=0.31$. From the table we can see that the first-order analytical solution overpredicts the friction coefficient a little; the LBM values are very close to the second-order predictions.

Third, micro-lid-driven cavity flow is investigated using the present LBM model. The cavity size is 300×300 (lattice units). The upper wall moves with a uniform constant velocity u_0 , from left to right and other three walls are stationary.

Figure 2 shows the Knudsen number effect on the velocity profiles through the cavity center. We can see that as the Knudsen number increases, the slip u velocity at the lower wall [Fig. 2(a)] and slip v velocity at the lateral walls [Fig. 2(b)] increase. Similar behaviors can also be observed if the tangential momentum accommodation coefficient decreases.

In Fig. 3 we plot the positions of the vortex center of the streamlines at various Knudsen numbers and momentum accommodation coefficients, respectively. The Reynolds number is fixed at $\text{Re}=0.3$. It can be seen that the x position of the vortex center remains at the vertical centerline while the

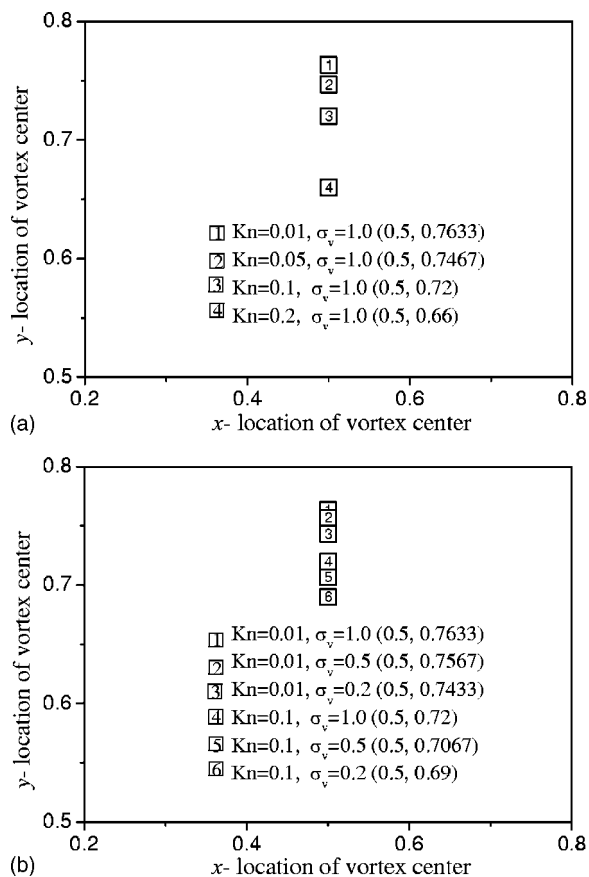


FIG. 3. The locations of the center of the vortex at $Re=0.3$. (a) The Knudsen number effect. (b) The tangential momentum accommodation coefficient effect.

y position moves downward as the Knudsen number increases or the momentum accommodation coefficient decreases.

To develop the lattice Boltzmann method for microflow investigation, the relation between the Knudsen number and the relaxation time is established and the slip velocity can be captured accurately using the discrete kinetic boundary conditions. Compared with bounce-back boundary condition commonly used in the lattice Boltzmann method, the present boundary condition will not increase the solving difficulty and it is still convenient to implement for complicated boundaries such that encountered in porous media flow. Although we use the two-dimensional nine-velocity model in

this Brief Communication, the approach can be directly applied to other velocity models and three-dimensional models. A detailed investigation for three-dimensional and micro-scale porous media flow will be reported in the future. In addition, compared with the traditional numerical methods for microflow simulation such as finite volume method employing slip boundary conditions, the computation effort of the lattice Boltzmann method maybe increases. However, it is much more computationally efficient than the molecular dynamics method or DSMC method.

This research was supported by the National Natural Science Foundation of China (Grant Nos. 50406020 and 50425620) and the National Key Project of Fundamental R&D of China (Grant No. G2000026303).

¹G. E. Karniadakis and A. Beskok, *Micro Flows: Fundamentals and Simulation* (Springer, New York, 2001).

²S. Y. Chen and G. D. Doolen, "Lattice Boltzmann method for fluid flows," *Annu. Rev. Fluid Mech.* **30**, 329 (1998).

³I. V. Karlin, A. Ferrante, and H. C. Ottinger, "Perfect entropy functions of the lattice Boltzmann method," *Europhys. Lett.* **47**, 182 (1999).

⁴S. Succi, I. V. Karlin, and H. D. Chen, "Colloquium: Role of the H theorem in lattice Boltzmann hydrodynamic simulations," *Rev. Mod. Phys.* **74**, 1203 (2002).

⁵S. Ansumali and I. V. Karlin, "Entropy function approach to the lattice Boltzmann method," *J. Stat. Phys.* **107**, 291 (2002).

⁶S. Ansumali and I. V. Karlin, "Single relaxation time model for entropic lattice Boltzmann methods," *Phys. Rev. E* **65**, 056312 (2002).

⁷S. Ansumali, I. V. Karlin, and S. Succi, "Kinetic theory of turbulence modeling: smallness parameter, scaling and microscopic derivation of Smagorinsky model," *Physica A* **338**, 379 (2004).

⁸W. G. Vincenti and C. H. Kruger, Jr., *Introduction to Physical Gas Dynamics* (Wiley, New York, 1965).

⁹D. P. Ziegler, "Boundary conditions for lattice Boltzmann simulations," *J. Stat. Phys.* **71**, 1171 (1993).

¹⁰G. H. Tang, W. Q. Tao, and Y. L. He, "Lattice Boltzmann method for simulating gas flow in microchannels," *Int. J. Mod. Phys. C* **15**, 335 (2004).

¹¹S. Ansumali and I. V. Karlin, "Kinetic boundary conditions in the lattice Boltzmann method," *Phys. Rev. E* **66**, 026311 (2002).

¹²R. Gatignol, "Kinetic theory boundary conditions for discrete velocity gases," *Phys. Fluids* **20**, 2022 (1977).

¹³C. Cercignani, *Theory and Applications of the Boltzmann Equations* (Scottish Academic, New York, 1975).

¹⁴L. Preziosi and E. Longo, "On the decomposition of domains in nonlinear discrete kinetic theory," in *Discrete Models of Fluids Dynamics, Advances in Mathematics for Applied Sciences*, edited by A. S. Alves (World Scientific, Singapore, 1991), Vol. 2, pp. 144–155.

¹⁵N. G. Hadjiconstantinou, "Comment on Cercignani's second-order slip coefficient," *Phys. Fluids* **15**, 2352 (2003).